

Spectroscopic Observations of the Comet 29P/ Schwassmann-Wachmann 1 at the SOAR Telescope

Oleksandra V. Ivanova^{a,b,*}, Enos Picazzio^c, Igor V. Luk'yanyk^d, Oscar Cavichia^e, Sergei M. Andrievsky^{f,g}

^a*Astronomical Institute of the Slovak Academy of Sciences, SK-05960 Tatranská Lomnica, Slovak Republic*

^b*Main Astronomical Observatory, National Academy of Sciences of Ukraine, Goloseevo, Kyiv, 03680 Ukraine*

^c*Universidade de São Paulo, Instituto de Astronomia, Geofísica e Ciências Atmosféricas, Departamento de Astronomia, Rua do Matão, 1226; Cidade Universitária, CEP 05508-900, São Paulo, SP, Brasil*

^d*Astronomical Observatory, Taras Shevchenko National University of Kyiv, Observatorna str. 3, Kyiv, 04053 Ukraine*

^e*Instituto de Física e Química, Universidade Federal de Itajubá, Av. BPS, 1303; Pinheirinho, CEP 37500-903, Itajubá, BRASIL*

^f*Department of Astronomy and Astronomical Observatory, Odessa National University, Shevchenko Park, 65014, Odessa, Ukraine*

^g*GEPI, Observatoire de Paris, PSL Research University, CNRS, Place Jules Janssen, 92195 Meudon, France*

Abstract

We carried out photometric and spectroscopic observations of comet 29P/Schwassmann-Wachmann 1 at the SOAR 4.1-meter telescope (Chile) on August 12, 2016. This paper presents the results of only spectroscopic analysis. The spectra revealed presence of CO⁺ and N₂⁺ emissions in the cometary coma at a distance of 5.9 AU from the Sun. The ratio [N₂⁺]/[CO⁺] within the projected slit seems to be 0.01. We have also estimated spectral gradient value for the comet.

Keywords: Comets; Comet 29P/Schwassmann-Wachmann 1; Spectroscopy; Centaurs.

*Corresponding author

Email address: sandra@mao.kiev.ua (Oleksandra V. Ivanova)

1. Introduction

Small bodies with orbits beyond Neptune orbit are of interest because they must have undergone minimal changes since the Solar System formation. Some comets show significant activity at distances far from the Sun. This is unusual since at the low equilibrium temperature (<140 K) the significant physical activity caused by the water ice sublimation is not expected. At the distances greater than 3 AU sublimation of CO and CO₂ ices may become the triggering mechanism producing the coma. Optical spectroscopy reveals the presence of the CO ions and CN radicals in the coma of comet 29P/Schwassmann-Wachmann 1 (hereafter SW1) (Cochran et al. 1991a; Cochran et al. 1980; Cochran et al. 1982; Cochran et al. 1991b; Cook et al. 2005; Larson 1980).

Current observational data (including Galileo space telescope data) indicate the high abundance of the metals (from astrophysical point of view, all elements heavier than helium) with respect to hydrogen in the giant planets atmospheres, and this value is much higher than that observed in the Sun. To explain this fact, the giant planets formation models require presence of accretion. The accreted material should contain the volatile components, such as neon, argon, krypton, xenon, which could not survive at the distance where giant planets were formed. Such a substance could be effectively delivered by the Oort Cloud and Kuiper Belt bodies, assuming that they were formed at temperatures below 30 K. This fact is supported by our observations of distant comets, after the emission line N₂⁺ was detected in two comets, C/2002 VQ94 (LINEAR) and SW1 (Korsun et al. 2006, 2008; Ivanova et al. 2016 and this work). New results obtained by Rubin et al. (2015), who investigated and detected the molecular nitrogen content in the nucleus of comet Churyumov-Gerasimenko using a mass spectrometer on board ROSINA probe "Rosetta", are also in agreement with that statement. According to modern understanding, the distant comets are members of the Kuiper Belt and Oort Cloud and therefore they should contain a pristine material from which the Solar System bodies were created. Abundance of this molecule may give us an important information about ice condensation in protosolar nebula and delivering of the volatile elements to the terrestrial planets.

In this work we investigate the comet SW1. SW1 is a distant comet and is regarded to be a comet of the centaurs class. The study of centaur is still hampered by limited physical data. Therefore, every new observation and

research of centaurs is important.

2. Observation and reduction

Spectrophotometric observations were made at the SOAR 4.1 m telescope in Cerro Pachón - Chile during August 12, 2016. The comet was observed at the heliocentric distance of 5.9 AU. The Goodman imaging/spectrograph was used with a 600 l/mm grid, which provides for the spectroscopic mode a reciprocal dispersion of 0.065 nm/pixel and, using a 1.68 arcsec slit width, a spectral element resolution of 0.73 nm. The SOAR Goodman spectrograph blue camera features one 4096 x 4096 pixel Fairchild CCD and a 7.2 arcmin in diameter field of view in the imaging mode. The seeing was stable during the night, with a mean value of 0.8 arcsec FWHM. The cometary spectra were acquired with 10 exposures of 1200 s each, which were co-added to increase the final signal-to-noise ratio. The spectrophotometric standard star LTT 9491 from Hamuy et al. (1992, 1994) was observed with a long slit of 3 arcsec width, allowing a more precise flux calibration. Cu-Ar arcs were taken immediately after each 3 exposures of cometary spectra in order to perform wavelength calibration. Data reduction was performed using the IRAF package, following the standard procedure for CCD reduction, i.e. correction of bias and flat-field. The spectral images were extracted and calibrated in wavelength and flux. Atmospheric extinction was corrected through mean coefficients derived for the CTIO observatory. Summarized information about the observations for SW1 is presented in Table 1.

[Table 1 about here.]

3. The spectroscopic data analysis

As we know the observed spectrum of a comet is a combination of the emission spectrum of the coma gas and the reflection spectrum of the dust coma.

$$F_{comet} = F_{gas} + F_{dust}, \quad (1)$$

The dust spectrum F_{dust} can be written as

$$F_{dust} = C(\lambda)F_{solar} \quad (2)$$

F_{solar} is the solar spectrum and $C(\lambda)$ is a function describing the reflectivity and scattering of the dust. In order to extract the gas emission spectrum F_{gas} from the observed cometary spectrum F_{comet} the function $C(\lambda)$ has to be determined. There are two ways to obtain the solar spectrum F_{solar} . The best way would be to observe the solar spectrum directly with the same instrumental setup as the comet. Also a practical solution is to observe a solar analog star. These stars are of the same spectral class as our Sun and have therefore a nearly identical spectrum. If the solar spectrum has not been observed in the same night, the solar spectral atlas by Kurucz et al. (1984) or Neckel & Labs (1984) can be used. We used the solar spectral atlas by Kurucz et al. (1984). That solar spectrum has very high resolution. For this reason it was convolved with a Gaussian profile to decrease the resolution and normalized to the flux of the comet around 5000 Å. The convolved solar spectrum is compared with the cometary spectrum in Fig. 1a. Solar absorption bands have to be identical in width and depth.

[Figure 1 about here.]

The approach chosen to obtain $C(\lambda)$ is to approximate the function by a polynomial $C(\lambda)$ or to interpolate by spline or to use the median filter with wide window after dividing the cometary spectrum by the solar one. We used solar absorption lines in comet and solar spectra as repers and spline approximation. The result is displayed in Fig. 1b. The spectrum $C(\lambda) \cdot F_{solar}$ together with the cometary spectrum is shown in Fig. 1c. This one is then subtracted from the cometary spectrum (Fig. 1d). Qualitative comparison curves on the panels in Fig. 1 indicates the presence of weak cometary molecular emissions and some differences on the flux distribution between the spectra.

The dust color indicates trends in the wavelength dependence of the light scattered by the dust. Traditionally the color of cometary dust was determined through measurements of the comet magnitude m in two different continuum filters. This color was a unitless characteristic expressed as the logarithm of the ratio of intensities in two filters. Although this definition is still used, spectrophotometry of comets resulted in the definition of color as the spectral gradient of reflectivity, usually measured in % per 1000 Å with an indication of the range of wavelength it was measured in.

From Fig. 1b, one can see that there is a nonlinear increase with the wavelength of the scattering efficiency in blue and red regions.

The spectral reflectance is $S(\lambda) = F_c(\lambda)/F_s(\lambda)$. Here, $F_c(\lambda)$ is the cometary continuum, and $F_s(\lambda)$ is a scaled spectrum of the Sun. The normalized reflection ability S' can be described as in Jewitt & Meech (1986):

$$S'(\lambda_1, \lambda_2) = \frac{\frac{dS}{d\lambda}}{S_{mean}}, \quad (3)$$

where $\frac{dS}{d\lambda}$ is the rate of change of the reflectivity with respect to wavelength in the region from λ_1 to λ_2 and S_{mean} is the mean reflectivity in the observed wavelength range:

$$S_{mean} = N^{-1} \sum S_i(\lambda). \quad (4)$$

In Ivanova et al. (2016) we determined the $S'(\lambda_1, \lambda_2)$ for the most typical spectral regions that are defined by the effective wavelengths of the cometary filters used for the continuum registration [BC (4430 Å), GC (5260 Å) and RC (6840 Å)], see (Schleicher & Farnham, 2004) as $11.4 \pm 2.3\%$ per 10^3 Å for the range 4430 - 5260 Å, $17.9 \pm 5.6\%$ per 10^3 Å for the range 5260 - 6840 Å and $14.8 \pm 4.8\%$ per 10^3 Å for the range 4430 - 6840 Å. The values obtained for the normalized spectral gradient for ranges 4430 - 5260 Å and 5260 - 6840 Å are comparable within the error bars to the redder wavelength region. This result does not allow an unambiguous conclusion about the normalized spectral gradient behavior with increasing wavelength.

Now we observed comet in spectral region 3300 - 5700 Å, therefore unfortunately we cannot use RC. But because we used the SOAR Goodman spectrograph blue camera, now we add UC (3448 Å) measurements. So we obtained the following results for the normalized spectral gradient: $7.80 \pm 0.02\%$ per 10^3 Å for the range 3448 - 4450 Å, $6.04 \pm 0.003\%$ per 10^3 Å for the range 4450 - 5260 Å and $3.87 \pm 0.02\%$ per 10^3 Å for the range 3448 - 5260 Å.

Like Ivanova et al. (2016) we made identification in the spectra of comet 29P. The SOAR Goodman spectrograph blue camera enabled us to investigate more shorter wavelengths of the spectrum, which is usually highly noisy. The linear spectrum of the comet is shown in Fig. 2. An identification of the spectra details was made by means of comparison with laboratory and calculated molecular spectra in the same spectral region.

[Figure 2 about here.]

The strongest features which extend along the whole observed spectral window are the comet-tail bands of CO^+ (Arpigny, 1964). Like in our previous investigation of Ivanova et al. (2016) the lines (2,0), (3,0), (2,0), (1,0), (5,1), (3,1), (2,1), (4,2), (3,2), (0,0), and (1, 1) of the vibrational transitions of CO^+ ($\text{A}^2\Pi\text{-X}^2\Sigma$) band system are clearly seen in Fig. 2. Additionally we have identified (6,0), (5,0) the vibrational transitions of CO^+ ($\text{A}^2\Pi\text{-X}^2\Sigma$) band system too. Two weak bands, (0, 1) and (1, 2), which belong to the ($\text{B}^2\Sigma\text{-A}^2\Pi$) system (Baldet & Johnson) of the CO^+ ion, are detected as well. The $\text{N}_2^+(0, 0)$ band of the ($\text{B}^2\Sigma\text{-X}^2\Sigma$) electronic system is shown too. Also the $[\text{N}_2^+]/[\text{CO}^+]$ ratio is estimated by us like in Ivanova et al. (2016). We used integrated intensities of the $\text{CO}^+(2, 0)$ and $\text{N}_2^+(0, 0)$ bands and the excitation factors of $7.0 \times 10^{-2} \text{ photons}\cdot\text{s}^{-1}\cdot\text{mol}^{-1}$ for the $\text{N}_2^+(0, 0)$ band (Lutz et al., 1993) and $3.55 \times 10^{-3} \text{ photons}\cdot\text{s}^{-1}\cdot\text{mol}^{-1}$ for the $\text{CO}^+(2, 0)$ band (Lutz et al., 1993; Magnani & A’Hearn, 1986). If only (2, 0) band column density of CO^+ is used, then $[\text{N}_2^+]/[\text{CO}^+]$ should be equal to 0.01. This is the upper limit because $\text{CO}^+(5,1)$ bands show double peaks, and the second peak coincides with N_2^+ band. In Ivanova et al. (2016) we estimated the available contamination of N_2^+ by $\text{CO}^+(5,1)$. This contamination is only 19%.

4. Discussions

Our previous result (Ivanova et al., 2016) does not allow an unambiguous conclusion about the normalized spectral gradient behavior with increasing wavelength. Now we can state that in the range 3448-5260 Å, the spectral gradient decreases (see Fig. 3).

[Figure 3 about here.]

Usually the reddening slope decreases towards the near-infrared (Jewitt & Meech, 1986; Kolokolova et al., 2004). But some local variations of colors have been observed in comae. The color depends on the size distribution of the grains and aggregates and on their refractive indices, mainly for grains larger than the wavelength. For instance, the jets of the Hale-Bopp comet were less red than background. It is possible that this effect was caused by the dust particle size less than one micron (Furusho et al., 1999). Comet C/1999 S4 (LINEAR) showed bluer color while the small dust grain were detected just after beginning of its disruption (Hadamcik & Levasseur-Regourd, 2003). Small-size dust grains (water ice crystals, for instance) can be responsible for

such a color. The rather transparent dust grains (water ice crystals, some silicates, or unaltered organic molecules) can be responsible for bluer color of the comet (Kiselev et al., 2004; Hadamcik & Levasseur-Regourd, 2009; Zubko et al., 2011, 2012; Hadamcik et al., 2014).

For five Jupiter-family comets, the average value is 19% per 10^3 \AA (Hadamcik & Levasseur-Regourd, 2009). We have calculated (Ivanova et al., 2016) the average value of the normalized spectral gradient for Centaurs (in Table 5 from Peixinho et al., 2015). The value of the normalized spectral gradient for the Centaurs is 21.3 ± 1.4 per 10^3 \AA . We found that the mean value of the normalized spectral gradient for SW1 is $5.9 \pm 0.03\%$ per 10^3 \AA and $14.7 \pm 4.2\%$ per 10^3 \AA . The observed change in the color of the comet SW1 (Fig.1) can be related to its degree of activity in the observed period.

Knowledge of the nitrogen content of comets is important for an understanding of conditions in the early solar nebula. Lewis & Prinn (1980) showed that conditions in the early solar nebula were such that the dominant equilibrium species of carbon, oxygen and nitrogen should be N_2 , CO, and H_2O .

It is expected that the most abundant species in the protoplanetary nebula (together with water ice) were CO and CO_2 ices (Meech & Svoren, 2004). The transitions of the CO^+ molecule identified in this work confirm this conclusion. According to Capria et al. (2000a,b) volatiles species can exist in the comet nuclei in the form of ices, as well as in the form of gaseous inclusions in amorphous water ice cells. CO sublimation begins at about 25 K (at large distances), while CO gas release from water ice cells begins at temperatures more than 100 K (Prialnik et al., 1995), i.e. at distances closer to the Sun.

N_2 molecule is rather inertious one, and therefore it is suitable to study nitrogen chemistry of comets, although observation of N_2 bands is a difficult task. As a result N_2 was detected only in some comets. For example, Cochran et al. (2000) report about non-detection of N_2 and clear detection of CO. They derived upper limits of N_2/CO of $3.0 \cdot 10^{-4}$ and 0.7 to $1 \cdot 10^{-4}$ for deVico and Hale-Bopp, respectively. The N_2/CO ratio is almost equal to the N_2^+/CO^+ ratio. These upper limits, compared to the NH_3 and CO abundances relative to water measured in comets, correspond to a very low abundance of N_2 in cometary ice. In comet Hale-Bopp, the N_2/NH_3 ratio is less than 0.001. Comparing with laboratory experiments on the deposition of various gases along with H_2O amorphous ice (Bar Nun et al., 1988), Cochran et al. (2000) concluded that N_2/CO is strongly depleted in these two comets. On the other hand, the N_2 depletion does not appear so great in other comets in which N_2 was possibly detected (see Table 3 from Cochran et al. 2000).

Cochran et al. (2000) discussed the results obtained in Comets deVico and Hale-Bopp and presented various arguments or speculations explaining the nitrogen depletion. They concluded that either a mechanism must be found to deplete the N_2 abundance in cometary ices after the formation of comets, or we have to understand how cometary icy grains depleted in N_2 may originate from a presolar cloud in which N_2 is currently estimated, according to the most chemical models of the interstellar medium, to be more abundant than NH_3 . However, Charnley & Rodgers (2002) showed that it is possible that much of the available nitrogen in the presolar cloud was in the form of atomic nitrogen N_2 , with a significant contribution in NH_3 ice, and little contribution in N_2 . This circumstance can explain apparent deficiency of N_2 seen in comets. Cochran (2002) used the high-resolution spectra to search for the N_2^+ bands but without success. Therefore, an upper limit of $5.4 \cdot 10^{-4}$ was set. To explain the strong depletion of N_2 one might suppose that the reason is the following: this molecule reluctantly form clathrate hydrates, in contrast with such molecule as CO. Last results obtained from the ROSINA mass spectrometer onboard of ROSETTA also detected molecular nitrogen in the nucleus of comet 67P/Churyumov-Gerasimenko. Possible mechanisms of ionization of the parent CO in cometary coma at large heliocentric distance are not fully understood, also. We detect both N_2^+ and CO^+ . We compare our estimate of N_2^+/CO^+ ratio with estimates by other authors and show the results in Fig. 4.

[Figure 4 about here.]

5. Conclusions

1. Spectral dependence of the light scattering by the cometary dust is obtained from the spectral observations of the comet SW1. The mean value of the normalized spectral gradient is $5.9 \pm 0.03\%$ per 10^3 \AA .
2. We detected numerous lines of CO^+ as well as the $N_2^+(0, 0)$ line of the ($B^2\Sigma-X^2\Sigma$) system, suggesting that the comet was formed in a low temperature (about 25 K) environment.
3. Additionally we have identified (6,0), (5,0) of the vibrational transitions of CO^+ ($A^2\Pi-X^2\Sigma$) band system also.
4. The value of $[N_2^+]/[CO^+]$ is equal to 0.01 for comet SW1.

Acknowledgements

This research is based on observations obtained at the Southern Astrophysical Research (SOAR) telescope, which is a joint project of the Ministério da Ciência, Tecnologia e Inovação (MCTI) da República Federativa do Brasil, the U.S. National Optical Astronomy Observatory (NOAO), the University of North Carolina at Chapel Hill (UNC), and Michigan State University (MSU). O. Ivanova thanks the SASPRO Programme, the People Programme (Marie Curie Actions) European Union's Seventh Framework Programme under REA grant agreement No. 609427, and the Slovak Academy of Sciences (grant Vega 2/0032/0014). I. Luk'yanyk research is supported by the project 16BF023-02 of the Taras Shevchenko National University of Kyiv and the Slovak Academy of Sciences (grant Vega 2/0032/0014).

References

- Arpigny, C. 1964, *Annales d'Astrophysique*, 27, 406.
- Capria, M. T., Coradini, A., De Sanctis, M. C., & Orosei, R., 2000a. CO emission mechanisms in C/1995 O1 (Hale-Bopp). *Astron. J.* 357, 359-366.
- Capria, M. T., Coradini, A., De Sanctis, M. C., & Orosei, R., 2000b. Chiron Activity and Thermal Evolution. *Astron. J.* 119, 3112-3118.
- Charnley, S.B., Rodgers, S.D., 2002. The end of interstellar chemistry as the origin of nitrogen in comets and meteorites. *Astrophys. J.* 569, L133L137.
- Cochran, A.L., Barker, E.S., Cochran, W.D., 1980. Spectrophotometric observations of 29P/Schwassmann-Wachmann 1 during outburst. *Astron. J.* 85, 474-477.
- Cochran, A.L., Cochran, W.D., Barker, E.S., 1982. Spectrophotometry of Comet Schwassmann-Wachmann 1. II. Its color and CO⁺ emission. *Astrophys. J.* 254, 816-822.
- Cochran, A.L., Cochran, W.D., 1991. The first detection of CN and the distribution of CO⁺ gas in the coma of Comet P/Schwassmann-Wachmann 1. *Icarus* 90, 172-175.

- Cochran, A.L., Cochran, W.D., Barker, E.S., Storrs, A.D., 1991. The development of the CO⁺ coma of Comet P/Schwassmann-Wachmann 1. *Icarus* 92, 179-183.
- Cochran, A.L., Cochran, W.D., Barker, E.S., 2000. N₂ and CO in Comets 122P/1995 S1 (deVico) and C/1995 O1 (HaleBopp). *Icarus* 146, 583-593.
- Cochran, A. L. 2002, A Search for N₂⁺ in Spectra of Comet C/2002 C1 (Ikeya-Zhang). *Astrophys. J.* 576, L165-L168.
- Cook, J.C., Desch, S.J., Wyckoff, S., 2005. Visible and near infrared spectra of Comet 29P/Schwassmann-Wachmann 1. *Bull. Am. Astron. Soc.* 37, 645 (abstract).
- Farnham, T. L., Schleicher, D. G., & A'Hearn, M. F. 2000. The HB Narrow-band Comet Filters: Standard Stars and Calibrations. *Icarus* 147, 180-204.
- Furusho, R., B. Suzuki, N. Yamamoto, H. Kawakita, T. Sasaki, Y. Shimizu, and T. Kurakami, 1999. Imaging polarimetry and color of the inner coma of comet Hale-Bopp (C/1995 O1). *Pub. Ast. Soc. Japan* 51, 367-473.
- Gautier, D., Hersant, F., Mousis, O., Lunine, J.I., 2001a. Enrichments in volatiles in Jupiter: a new interpretation of the Galileo measurements. *Astrophys. J.* 550, L227-L230.
- Gautier, D., Hersant, F., Mousis, O., Lunine, J.I., 2001b. Erratum: enrichments in volatiles in Jupiter: a new interpretation of the Galileo measurements. *Astrophys. J.* 559, L183-L183.
- Hadamcik, E. and Levasseur-Regourd, A.-C., 2003. Dust coma of comet C/1999 S4 (LINEAR): Imaging polarimetry during nucleus disruption. *Icarus* 166, 188-194.
- Hadamcik, E. and A. C. Levasseur-Regourd 2009. Optical properties of dust from Jupiter Family comets. *Plan. Space Sci.* 57, 1118-1132.
- Hadamcik, E., J.-B. Renard, A. Buch, N. Carrasco, N. Johnson, and J. Nuth, 2014. Linear polarization of light scattered by cometary analogs: New samples. *Asteroids, Comets, Meteors 2014* Helsinki, Finland.
- Hamuy, M., Walker, A. R., Suntzeff, N. B., et al., 1992, Southern spectrophotometric standards, *PASP* 104, 533.

- Hamuy, M., Suntzeff, N. B., Heathcote, S. R., et al., 1994, Southern spectrophotometric standards, 2, PASP 106, 566.
- Iro, N., Gautier, D., Hersant, F., Bockelée-Morvan, D., & Lunine, J. I. 2003, Icarus 161, 511-532.
- Ivanova O. V., Luk'yanyk I. V., Kiselev N. N., Afanasiev V. L., Picazzio E., Cavichia O., de Almeida A. A., Andrievsky S. M., 2016. Photometric and spectroscopic analysis of Comet 29P/Schwassmann-Wachmann 1 activity, Planet. Space Sci. 121, 10-17.
- Jewitt D. and Meech K. J., 1986. Cometary grain scattering versus wavelength, or, what color is comet dust? Astrophys. J. 310, 937-952.
- Kolokolova, L., Hanner, M. S., Lvasseur-Regourd, A. C., Gustafson, B. A. S., 2004, in Comets II, ed. M. C. Festou, H. U. Keller, H. A. Weaver (Tucson: Univ. Arizona Press), P. 577-604.
- Korsun, P. P., Ivanova, O. V., & Afanasiev, V. L. 2006. Cometary activity of distant object C/2002 VQ94 (LINEAR). Astron. Astrophys., 459(3), 977-980.
- Korsun, P.P., Ivanova, O.V., Afanasiev, V.L., 2008. C/2002 VQ94 (LINEAR) and 29P/Schwassmann-Wachmann 1 CO⁺ and N₂⁺ rich comets. Icarus 198, 465-471.
- Kiselev, N. N., K. Jockers, and T. Bonev, 2004. CCD imaging polarimetry of comet 2P/Encke. Icarus 168, 385-391.
- Kurucz, R. L., Furenlid, I., Brault, J., & Testerman, L., 1984, Solar flux atlas from 296 to 1300 nm. National Solar Observatory Atlas, Sunspot, New Mexico: National Solar Observatory, 1984.
- Landolt, A. U., 1992. UBVRI photometric standard stars in the magnitude range 11.5-16.0 around the celestial equator. Astron. J. 104, 340-371.
- Larson, S.M., 1980. CO⁺ in Comet Schwassmann-Wachmann 1 near minimum brightness. Astrophys. J. 238, 47-48.
- Lewis, J. S., & Prinn, R. G. 1980, Kinetic inhibition of CO and N₂ reduction in the solar nebula. Astrophys. J. 238, 357-364.

- Lutz B. L., Womack M., Wagner R. M. Ion abundances and implications for photochemistry in Comets Halley (1986 III) and Bradfield (1987 XXIX), 1993. *Astrophys. J.* 407, 402-411.
- Magnani, L., & A'Hearn, M. F. 1986. CO⁺ Fluorescence in Comets. *Astrophys. J.* 302, 477-487
- Meech K.J., Svoren J. 2004 Using cometary activity to trace the physical and chemical evolution of cometary nuclei. In *Comets II* (eds MC Festou, HU Keller, HAWeaver), pp. 317-335. Tucson, AZ: University of Arizona Press.
- Meech K. J., 2017, Setting the scene: what did we know before Rosetta? *Philosophical Transactions of the Royal Society of London Series A*, 375, 20160247 DOI: 10.1098/rsta.2016.0247.
- Neckel, H., Labs, D., 1984. The solar radiation between 3300 and 12500 Å. *Sol.Phys.* 90, 205-258.
- Peixinho, N., Delsanti, A., Doressoundiram, A. 2015. Reanalyzing the visible colors of Centaurs and KBOs: what is there and what we might be missing, *Astron. Astrophys.*, 577, A35
- Prialnik, D., Brosch, N., & Ianovici, D., 1995. Modelling the activity of 2060 Chiron. *Month. Not. of RAS* 276, 1148-1154.
- Rubin, M., Altwegg, K., Balsiger, H., Bar-Nun, A., Berthelier, J. J., Bieler, A., ... & De Keyser, J., 2015. Molecular nitrogen in comet 67P/Churyumov-Gerasimenko indicates a low formation temperature. *Science*, 348(6231), 232-235.
- Schleicher D. G. and Farnham T. L., 2004. In *Comets II*, Ed. by M. Festou, H. U. Keller, and H. A. Weaver (The University of Arizona Press, Tucson), pp. 449-470.
- Zubko, E., R. Furusho, K. Kawabata, T. Yamamoto, K. Muinonen, and G. Videen, 2011. Interpretation of photopolarimetric observations of comet 17P/Holmes. *J. Quant. Spectrosc. Radiat. Transfer* 112, 1848-1863.
- Zubko, E., K. Muinonen, Y. Shkuratov, E. Hadamcik, and A. C. Levasseur-Regourd 2012. Evaluating the carbon depletion found by the Stardust mission in comet 81P/Wild 2. *Astr. and Ap.* 544, L8.

List of Figures

1	The results of processing of the spectrum of comet 29P/Schwassmann-Wachmann 1: (a) the energy distribution in the comet's spectrum (black line) and the shifted normalized spectrum of the Sun (gray line); (b) the normalized spectral dependence of the reflectivity of dust; (c) the spectrum of the comet (black line) and the calculated comet's continuum (gray line); (d) the emission component in the comet's spectrum.	14
2	Molecular emissions identified in the observed spectrum of comet SW1. Calculated spectra of the identified species are displayed at the bottom of the figure.	15
3	Behavior of the spectral gradient for comet SW1. ● - this work; △ - from Ivanova et al. (2016)	16
4	Estimates of $N_2^+(0,0)/CO^+(4,0)$ for different comets. a - is semi-major axis; × - 29P/SW1 (this work and Ivanova et al. 2016; we converted the intensity ratios by using the relationship $I(4, 0) = 0.6 \times I(2, 0)$, where $I(4, 0)$ is the intensity of the (4,0) band, $I(2, 0)$ is the intensity of the (2,0) band, and the factor is taken from Table 4 of Magnani & A'Hearn 1986); ● - from table 3 of Cochran et al. 2000; + - from Cochran 2002 and Cochran et al. 2000	17

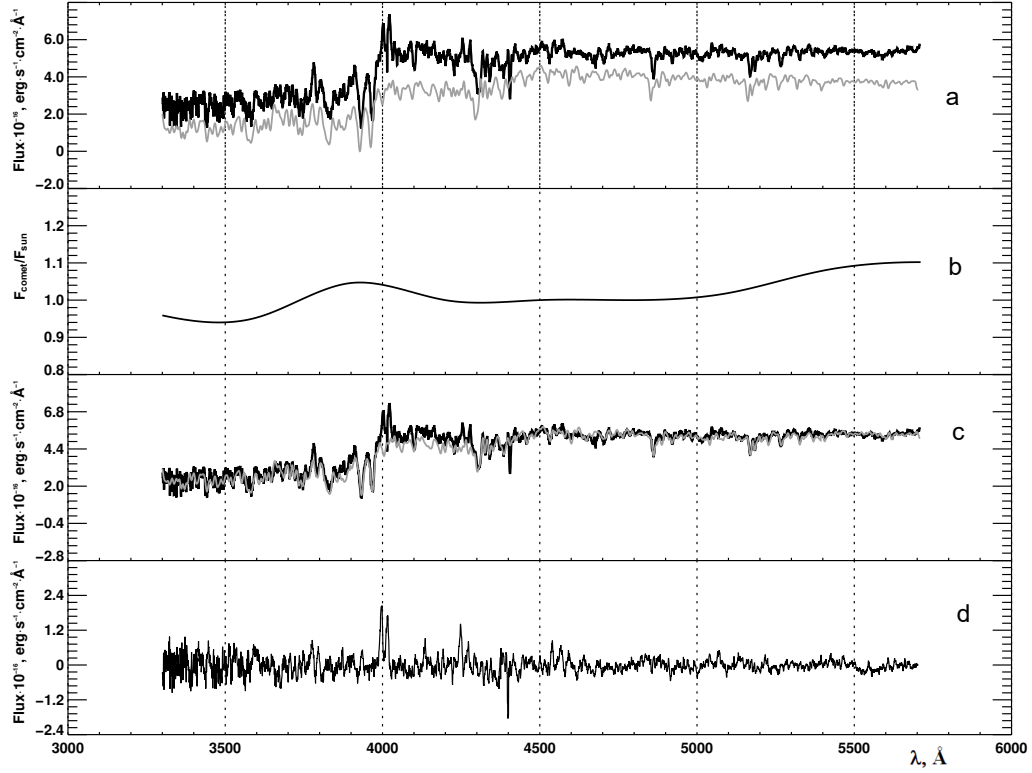


Figure 1: The results of processing of the spectrum of comet 29P/Schwassmann-Wachmann 1: (a) the energy distribution in the comet's spectrum (black line) and the shifted normalized spectrum of the Sun (gray line); (b) the normalized spectral dependence of the reflectivity of dust; (c) the spectrum of the comet (black line) and the calculated comet's continuum (gray line); (d) the emission component in the comet's spectrum.

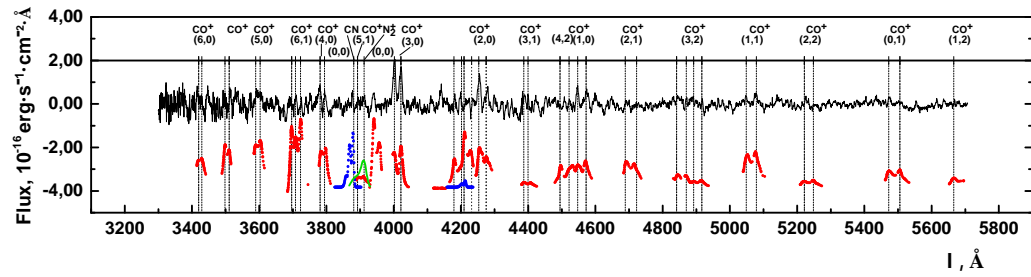


Figure 2: Molecular emissions identified in the observed spectrum of comet SW1. Calculated spectra of the identified species are displayed at the bottom of the figure.

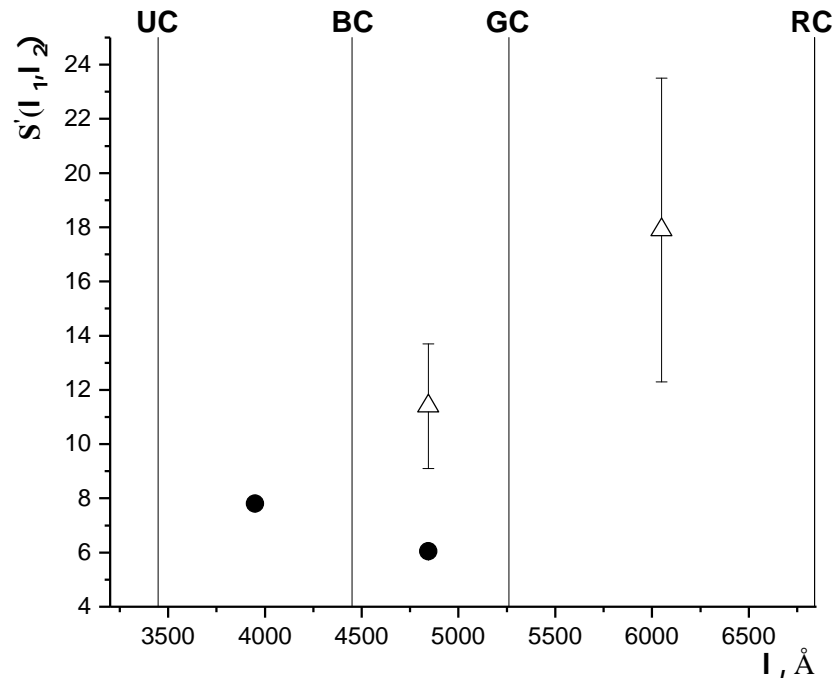


Figure 3: Behavior of the spectral gradient for comet SW1. ● - this work; △ - from Ivanova et al. (2016)

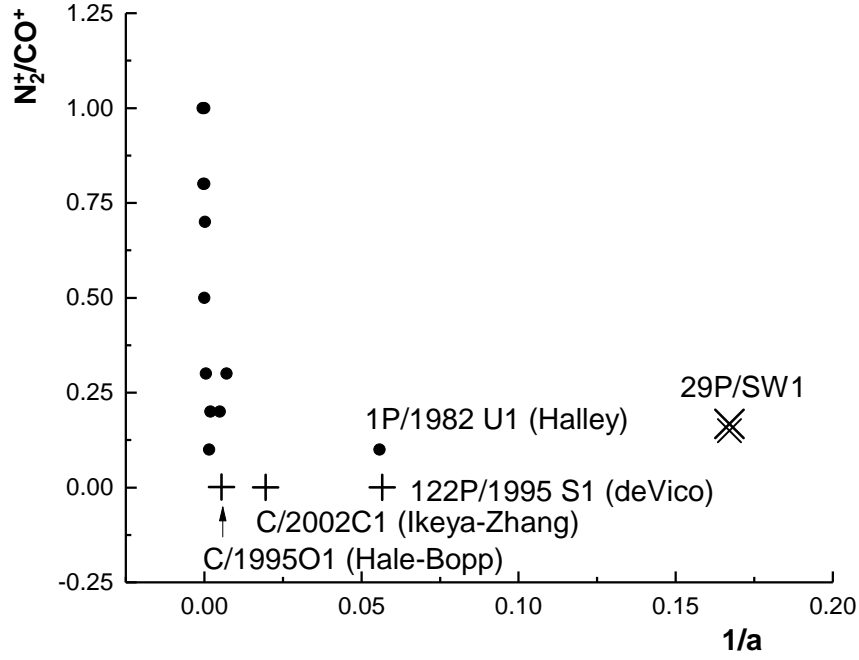


Figure 4: Estimates of $N_2^+(0,0)/CO^+(4,0)$ for different comets. a - is semi-major axis; \times - 29P/SW1 (this work and Ivanova et al. 2016; we converted the intensity ratios by using the relationship $I(4, 0) = 0.6 \times I(2, 0)$, where $I(4, 0)$ is the intensity of the (4,0) band, $I(2, 0)$ is the intensity of the (2,0) band, and the factor is taken from Table 4 of Magnani & A'Hearn 1986); \bullet - from table 3 of Cochran et al. 2000; $+$ - from Cochran 2002 and Cochran et al. 2000

List of Tables

1	Log of the observations of comet 29P/Schwassmann-Wachmann	
1	19

Table 1: Log of the observations of comet 29P/Schwassmann-Wachmann 1

Date of observ. (UT)	Exptime, (s)	r, (AU)	Δ , (AU)	α , ^a (°)	Type	Info ^b
2016 Aug. 12	1200	5.9	5.0	5.1	Spec.	7.28 Å
	300					B
	200				Phot	V
	100					R
	100					I

^aPhase angle.

^bSpectral resolution and filter used.